CUME EXAM # 359

This exam is worth 85 points. It is based on the accompanying paper by Bauer et al. (2010), "Direct detection of seasonal changes on Triton with Hubble Space Telescope" Astrophys. J. Let. 723, L49-L52. A grade of 65% or higher is expected to be a passing grade.

Things You Might Need to Know

1 AU =
$$1.496 \times 10^{13}$$
 cm
1 Joule = 10^7 erg
 $G = 6.674 \times 10^{-8}$ dyn cm² g⁻²
 $c = 2.9979 \times 10^{10}$ cm s⁻¹
 $k = 1.3806 \times 10^{-16}$ erg K⁻¹
mass of unit atomic weight $(m_{amu}) = 1.660 \times 10^{-24}$ g
Universal gas constant $(R_{univ}) = 8.314 \times 10^7$ erg/mole/K
 c_p (air) = 1.004 J g⁻¹ K⁻¹
 $\sigma = 5.670 \times 10^{-5}$ erg cm⁻² K⁻⁴ s⁻¹

Parameter	Earth	Moon	Neptune	Triton
OSA*		$3.844 \times 10^5 \mathrm{\ km}$	30.07 AU	$3.5476 \times 10^{5} \; \mathrm{km}$
orbital period	₹, *	27.321 days		5.877 days
rotational period			16.11 hr	995.
radius (km)	6371	1737.5	24,766**	1352.6
mass	$5.974 \times 10^{24} \text{ kg}$	$7.349 \times 10^{25} \text{ g}$	$1.024 \times 10^{26} \text{ kg}$	$2.147 \times 10^{25} \; \mathrm{g}$
Bond albedo	0.29	0.123	0.31	

^{*} orbital semi-major axis

Orbital Mechanics

1. Calculate the semimajor axis of a moon on a synchronous orbit around Neptune. Express your answer in Neptune radii (R_N) from the center of the planet. Compare this distance with the orbit of Triton. Ignoring the fact that Triton has a retrograde orbit (i.e. pretend that it orbits Neptune in the prograde direction), describe the motion of Triton on the sky as seen from Neptune. (10 points)

Use Kepler's Third Law to solve this problem:

$$P^2 = \frac{4\pi^2}{G(M_N + M_T)} a^3 \tag{1}$$

^{**} equatorial radius

1

$$a = \left(\frac{G(M_N + M_T)P^2}{4\pi^2}\right)^{1/3} \tag{2}$$

Since $M_N \sim 4800 \times M_T$,

$$a \sim \left(\frac{GM_N P^2}{4\pi^2}\right)^{1/3} \tag{3}$$

A satellite in a synchronous orbit around Neptune will have an orbital period equal to that of Neptune's rotational period, so

$$a = \left(\frac{(6.67 \times 10^{-11} m^3 kg^{-1}s^{-2})(1.024 \times 10^{26} kg)(16.11 \times 3600s)^2}{4\pi^2}\right)^{1/3},\tag{4}$$

yielding $a=8.35\times 10^7$ m = 3.4 R_N . From the information provided in the table, Triton's OSA is 14.3 R_N . Thus, its orbital period is $\sim 4\times$ longer than that required for a synchronous orbit. This means that as seen from Neptune (if we were to assume that Triton orbits in the prograde direction), Triton will rise in the east and set in the west, just as our Moon does.

2. Compute the ratio of the differential tidal force on Triton due to Neptune to the differential tidal force on the Moon due to the Earth. (10 points)

The general expression for tidal force is given by

$$\Delta F = \frac{2GMmR}{a^3},\tag{5}$$

where M is the mass of one object, m is the mass of the second object, R is the radius of the object being deformed due to tidal forces, and a is the average distance between the centers of the two objects. Thus, the differential tidal force on Triton due to Neptune is given by the expression

$$\Delta F_T = \frac{2GM_N m_T R_T}{a_T^3} \tag{6}$$

where M_N is the mass of Neptune, m is the mass of Triton, R_T is Triton's radius, and a_T is Triton's orbital semimajor axis. Similarly, the differential tidal force on the Moon due to the Earth is

$$\Delta F_M = \frac{2GM_{\oplus}m_M R_M}{a_M^3} \tag{7}$$

The ratio of these two expressions is given by

$$\frac{\Delta F_{Triton}}{\Delta F_{Moon}} = \left(\frac{M_N}{M_{\oplus}}\right) \left(\frac{m_T}{m_M}\right) \left(\frac{R_T}{R_M}\right) \left(\frac{a_M}{a_T}\right)^3 \tag{8}$$

$$= \left(\frac{1.024 \times 10^{26}}{5.974 \times 10^{24}}\right) \left(\frac{2.147 \times 10^{25}}{7.349 \times 10^{25}}\right) \left(\frac{1352.6}{1735.5}\right) \left(\frac{3.844 \times 10^5}{3.5476 \times 10^5}\right)^3 = 4.97 \tag{9}$$

So the differential tidal force that Neptune exerts on Triton is $\sim 5 \times$ that exerted on the Moon by the Earth.

Radiation

3. Neptune radiates more than twice the radiation that it receives from the Sun. If Neptune's excess radiation comes from gravitational potential energy due to the slow, global contraction of the planet, at what rate (dR/dt) is Neptune shrinking in radius? Assume for this calculation that Neptune is of uniform density. At this rate of shrinkage, how long would it take for Neptune's radius to decrease by 1%? Compare this to the age of the solar system. (15 points)

The gravitational potential energy, U, is given by

$$U = -\frac{GM_r m}{r} \tag{10}$$

or

$$U = -G \int_0^m \frac{M_r dm}{r} \tag{11}$$

We consider the case for a spherical shell of thickness dr and integrate that over the size of the planet. The mass interior to the shell will be $M_r = \frac{4}{3}\pi r^3 \rho$, so we differentiate that to get $dm = 4\pi r^2 \rho dr$. The density ρ is just total mass/total volume, or $3M_N/4\pi R_N^3$. Then we can rewrite the above integral as

$$U = -G(\frac{4}{3}\pi\rho)(4\pi\rho)\int_0^{R_N} \frac{r^3r^2}{r} dr = -\frac{16G\pi^2\rho^2}{3}\int_0^{R_N} r^4 dr$$
 (12)

Completing this integration yields

$$-\frac{16G\pi^2\rho^2}{15}R_N^5\tag{13}$$

and substituting in our expression for ρ yields

$$-\frac{16}{15}\pi^2 G R_N^5 \left(\frac{9}{16} \frac{M_N^2}{\pi^2 R_N^6}\right) \tag{14}$$

$$U = -\frac{3}{5} \frac{GM_N^2}{R_N} \tag{15}$$

As the planet contracts the mass does not change, so the decreasing radius results in a decreasing gravitational potential energy:

$$\frac{dU}{dt} = \frac{3}{5} \frac{GM^2}{R^2} \frac{dR}{dt} \tag{16}$$

The contraction rate of the planet is thus given by

$$\frac{dR}{dt} = \frac{5}{3} \frac{dU}{dt} \frac{R^2}{GM^2} \tag{17}$$

The Sun's luminosity is 3.8×10^{26} W (sorry I forgot to give you that - thank you for asking for it). The rate at which Neptune absorbs energy from the Sun is given by:

$$F = \frac{L_{\odot}}{4\pi a_N^2} (1 - A_N) \pi R_N^2 \tag{18}$$

Then

$$F = \frac{(3.8 \times 10^{26} \ W)}{4\pi (30.07 \times 1.496 \times 10^{11} \ m)^2} (1 - 0.3)\pi (2.4766 \times 10^7 \ m)^2 = 2.0 \times 10^{15} \ W \quad (19)$$

So Neptune radiates away roughly twice the above value, or $\sim 4 \times 10^{15}~W$. Now we can compute Neptune's rate of contraction:

$$\frac{dR}{dt} \approx \frac{5}{3} (-4 \times 10^{15} \ J \ s^{-1}) \frac{(2.4766 \times 10^7 \ m)^2}{(6.67 \times 10^{-11})(1.024 \times 10^{26} \ kg)^2}$$
(20)

$$\frac{dR}{dt} \approx -5.8 \times 10^{-12} \ m \ s^{-1} \tag{21}$$

At this rate of shrinkage, for Neptune to shrink in radius by 1% it would take $(0.01 \times 2.4766 \times 10^7 m)/(5.8 \times 10^{-12} \ m\ s^{-1}) = 4.3 \times 10^{16} \ s \sim 1.4$ Gyr. This is roughly a third of the age of the solar system.

4. Confirm the following claim in the second paragraph of the paper: The average sub-solar ice temperature over Triton's disk is near 36.5 ± 1.5 K (Grundy & Young 2004), but with reflectance variations between 0.9 and 0.7 (Hillier et al. 1994), localized dark areas receive a threefold increase in energy from the average surface that can increase the temperature to 42 K. In other words, demonstrate that the quoted reflectance variations can result in the observed surface temperature deviations. (10 points)

Use the energy balance equation to relate reflectance variations and temperature. We need to equate the incoming solar flux to the outgoing thermal radiation:

$$F_{in} = \frac{L_{\odot}}{4\pi a_T^2} (1 - A_b) \pi R_T^2 \tag{22}$$

$$F_{out} = 4\pi R_T^2 \sigma T_e^4 \tag{23}$$

where A_b is the Bond albedo and T_e is Triton's effective temperature. Equating F_{in} and F_{out} and solving for T_e , we get

$$T_e = \left[\frac{L_{\odot} (1 - A_b)}{16\pi \sigma a_T^2} \right]^{1/4} \tag{24}$$

The only thing that changes in Eq. (24) is A_b , so we can ignore all of the other constants by lumping them into some new constant, X, and look at the ratio of the temperatures for the two different albedo values:

$$T(0.9) = [X(1 - 0.9)]^{1/4}$$
(25)

$$T(0.7) = [X(1-0.7)]^{1/4}$$
(26)

$$\frac{T(0.9)}{T(0.7)} = \left(\frac{0.1}{0.3}\right)^{1/4} = 0.76\tag{27}$$

The average surface temperature is 36.5, and if the surface reflectance (albedo) changed from 0.9 to 0.7, this would result in a temperature of the darker areas of 36.5/0.76 = 48 K. This is somewhat larger than the quoted temperature of 42 K, but at least it seems plausible. One factor that could influence this calculation and make it more complicated is the surface emissivity, which we have assumed = 1 in this simplified case. Another issue is Triton's rotational period; since it rotates slowly ($P_{rot} = P_{orb} = 5.88$ days), local surface albedo variations play a larger role.

Observations

- 5. The paper states that HST had the best optical resolution available for imaging Triton. What if the authors had wanted to observe Triton in K-band, a spectral region where there is significant methane absorption? Is it still true that HST would be the best option? To answer this question, address the following:
 - a) Calculate the diffraction limit in K-band for one of the Keck telescopes. Use your result, along with the plate scale for the NIRC2 narrow camera on Keck II (0.009942 "/pix), to determine the number of resolution elements you would have across Triton. (5 points)

The diffraction limit, or the minimum angular separation that can be resolved by a telescope, is

$$\theta_{min} = 1.22 \frac{\lambda}{D} \tag{28}$$

For one of the Keck telescopes (D = 10 m) at K band ($\lambda = 2.2 \mu m$), $\theta_{min} = 1.22$ (2.2 $\times 10^{-6}$ m)/(10 m) = 2.4 $\times 10^{-7}$ rad = 0.05". The NIRC2 plate scale thus oversamples the diffraction limit by a factor of ~ 5 . The paper states that Triton has an angular diameter of "nearly 0.13 arcsec," so even with diffraction-limited observations, one would have less than 3 (~ 2.6) resolution elements across Triton's disk in K-band.

b) Now consider using the ALTAIR adaptive optics (AO) system in conjunction with the NIRI imager on the Gemini telescope. The smallest plate scale on NIRI without the use of AO is 0.022. If the ALTAIR + NIRI system were used for K-band imaging of Triton, how many resolution elements would you have across Triton's disk? State whatever assumptions you make about the performance of the AO system. (5 points)

For the Gemini (8.1-meter) telescope, the diffraction limit $\theta_{min} = 1.22$ (2.2×10⁻⁶ m)/(8.1 m) = 3.3 ×10⁻⁷ rad = 0.068". Again we see that the NIRI plate scale oversamples the diffraction limit, this time by a factor of about 3. If you assume that the ALTAIR AO system worked *perfectly*, *i.e.* it enabled you to obtain diffraction-limited images, you would be able to obtain ~ 2 resolution elements across Triton's disk.

Planetary Atmospheres

6. What is the gravitational acceleration, g, at the surface of Triton? (5 points)

$$g_T = \frac{GM_T}{r_T^2} = \frac{(6.67 \times 10^{-11})(2.147 \times 10^{22} \ kg)}{(1.353 \times 10^6 \ m)^2} = 0.78 \ m \ s^{-2}$$
 (29)

7. If you approximate the atmosphere of Triton as consisting only of molecular nitrogen, what is the scale height of Triton's atmosphere? (10 points)

We start with a slab of atmosphere that we assume is in hydrostatic equilibrium to relate pressure and height. If it is in hydrostatic equilibrium, then the net forces acting on the slab must balance. The force downward is the gravitational force: $F_g = \Delta mg$. Density is mass/volume, so mass can be rewritten as density \times volume. So $F_g = g \rho \Delta A \Delta z$.

The upward force on the slab is the difference between the upward pressure force acting on the bottom of the slab and the downward pressure force acting on the top of the slab. The upward pressure foce acting on the bottom of the slab is force/area, so $F_{up} = p(z)\Delta A$. The downward pressure force acting on the top of the slab is $F_{down} = p(z + \Delta z)\Delta A$.

Balancing forces, we get

$$g\rho\Delta A\Delta z = p(z)\Delta A - p(z + \Delta z)\Delta A \tag{30}$$

Cancelling all the ΔA 's and expanding $p(z + \Delta z)$ into $p(z) + \frac{dp}{dz} \Delta z$ (using a Taylor expansion), we end up with the final expression

$$\frac{dp}{dz} = -\rho g. (31)$$

Now we need to add in an equation of state to relate pressure to temperature and density. For a planetary or brown dwarf atmosphere, we can use the ideal gas law, P = NkT = ρ kT/ μ , where N is the number density of molecules in the atmosphere, ρ is their mass density, k is Boltzmann's constant, and μ is the mean molecular weight of an atmosphere. Solving the above expression for ρ and plugging that back into our expression for hydrostatic equilibrium, we get

$$\frac{dp}{p} = -\frac{\mu g}{kT}dz\tag{32}$$

If you integrate both sides to get the variation of pressure with height, you end up with

$$p(z) = p(z_o)exp\left[-\frac{\mu g}{kT}(z - z_o)\right], \text{ or}$$
(33)

$$p(z) = p(z_o)exp\left[-\frac{(z-z_o)}{H}\right]$$
(34)

where $H \equiv \frac{kT}{\mu g}$ is the scale height, or the height over which the pressure falls by 1/e. Note: the assumptions inherent in these calculations are that the local acceleration of gravity, the temperature, and the chemical composition (μ) do not vary over the region of interest.

 μ is the mean molecular weight, which we must determine for an N₂ atmosphere. The mass of a nitrogen atom (in a.m.u.) ~ 14 . Thus, $m_{N_2} = 1.00 \ (2 \times 14) = 28$. So $\mu = 28 \times$ the mass of unit atomic weight, or $28 \times 1.660 \times 10^{-24}$ g.

Thus, H =
$$(1.38 \times 10^{-16} \text{ erg/K})(38 \text{ K})/(28 \times 1.660 \times 10^{-24} \text{ g})(78 \text{ cm/s}^2) = 14.5 \text{ km}$$
.

8. An atmosphere's exobase is the point in the atmosphere where a gas particle moving upward faster than the escape velocity is able to escape from the atmosphere before colliding with another particle. The temperature of Triton's exobase is ~ 100 K and it is at an altitude of ~ 930 km. Given a loss rate of Triton's atmosphere of 7×10^6 kg/year, and given a current surface pressure of 20 μ bar, calculate a "lifetime" for Triton's atmosphere and compare this number to the age of the solar system. Can this tell you anything about surface sources of N_2 ? (15 points)

We can determine the mass of Triton's atmosphere from its surface pressure; the force

of the entire atmosphere on Triton's surface is $F = P_o \times A = Mg$, where A is the surface area of Triton, P_o is the atmospheric surface pressure, and g is the gravitational acceleration at Triton's surface. Thus,

$$M = \frac{4\pi R_T^2 P_o}{g} \tag{35}$$

First, convert the surface pressure to a mks unit using 1 bar = 10^5 Pa = 10^5 N m⁻². So $P_o = 2$ Pa. Then

$$M = \frac{4\pi (1.353 \times 10^6 \ m)^2 (2 \ N \ m^{-2})}{0.78 \ m \ s^{-2}} = 5.9 \times 10^{13} \ kg \tag{36}$$

Given a loss rate of 7×10^6 kg/year, this means that Triton's atmosphere should escape within 8.4 million years, which is significantly less than the age of the solar system (4.5 billion years). This suggests that there must be a surface or sub-surface source of N_2 that is replenishing Triton's atmosphere.

Extra Credit/Bonus Problem

- 9. The paper states that the phase angle interval over which the observations were taken was external to Triton's narrow opposition surge.
 - a) Draw a diagram illustrating what this phase angle is (i.e. how it is defined). (2 points)

The phase angle is the Sun-Target-Observer angle. If the phase angle is 0°, then the Sun is directly behind you and the object you are observing is fully illuminated.

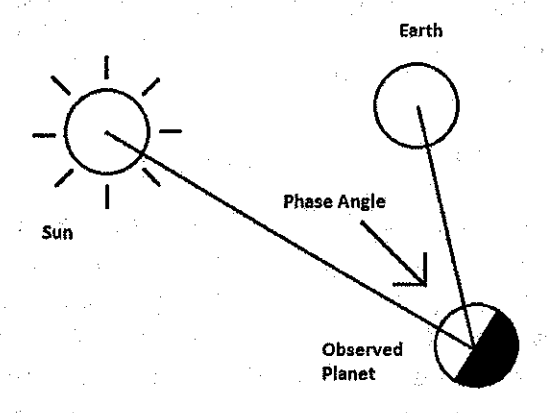


Figure 1: From http://upload.wikimedia.org/wikipedia/commons/1/10/Phase_Angle_3.jpg.

b) What is the "opposition surge" mentioned in the paper? (2 points)

The reflected brightness of many solar system bodies increases sharply as the phase angle approaches zero. This brightness increase at low solar phase angles is called the opposition surge, or sometimes the opposition effect. Most particulate surfaces as well as planetary rings exhibit an opposition effect. Two processes have been proposed to account for the phenomenon: the shadow-hiding opposition effect (SHOE), in which particles effectively block their own shadows as the phase angle approaches 0°, and the coherent backscatter opposition effect (CBOE), which is due to the constructive interference of multiply-scattered photons at small phase angles. The amplitude of the SHOE is directly proportional to particle opacity, and the angular width of the SHOE is related to the porosity of the surface and the distribution of grain sizes. These are affected by composition and by the thermal and collisional history of a body. Thus, a detailed characterization of the opposition effect can elucidate important surface properties as well as the evolutionary history of a planetary surface.

#	Pts.	Point Distribution				
	5 pts for correct use of Kepler's 3^{rd} Law (getting correct value for a)					
1	2 pt for recognizing that $P = Neptune's P_{rot}$ for synchronous orbit					
		1 pt for comparison with Triton's actual orbital semimajor axis				
		2 pts for describing what would orbit would look like from Neptune				
		6 pts for knowing correct expression for tidal force				
2	10	3 pts for computing values correctly for Triton and the Moon				
		1 pt for comparison between the two results (ratio)				
		4 pts for computing Neptune's radiation, 8 pts for computing rate of				
3	contraction, 2 pts for computing time required to shrink by 1%,					
		1 point for comparing to age of solar system				
4	10	5 pts for using correct equation, 5 pts for interpretation				
		3 pts for using correct equation, 1 pt for knowing size of Keck				
5(a)	5	telescope and wavelength of K band, 1 pt for computing correct				
		number of resolution elements				
5(b)	5	2 pts for using correct equation, 1 pt for using correct values,				
		2 pts for valid assumptions about performance of AO system				
6	5	3 pts for using correct equation, 2 pts for getting correct value				
7	10	5 pts for using correct equation, 3 pts for figuring out μ for an				
		N ₂ atmosphere, 2 pts for getting correct value				
8	15	8 pts for getting mass of atmosphere, 4 pts for computing lifetime				
		of atmosphere, 3 pts for discussion of replenishment source(s)				
9(a)	2	1 pt for correct identification of 3 bodies involved, 1 pt for				
		identifying the correct angle				
9(b)	2	1 pt for knowing it takes place when $\phi \to 0$, 1 pt for knowing				
		that it results in a brightness increase				

DIRECT DETECTION OF SEASONAL CHANGES ON TRITON WITH HUBBLE SPACE TELESCOPE

James M. Bauer¹, Bonnie J. Buratti¹, Jian-Yang Li², Joel A. Mosher¹, Michael D. Hicks¹, Britney E. Schmidt³, and Jay D. Goguen¹

¹ Jet Propulsion Laboratory, California Institute of Technology, 4800 Oak Grove Drive, MS 183–401, Pasadena, CA 91109, USA; bauer@scn.jpl.nasa.gov, Bonnie.Buratti@jpl.nasa.gov, jam@joelmosher.com, hicksm@scn.jpl.nasa.gov, jdg@scn.jpl.nasa.gov
² University of Maryland, Department of Astronomy, College Park, MD 20742, USA; jyli@astro.umd.edu

³ University of California, Los Angeles, Institute of Geophysics & Planetary Physics, 2240 1/2 S Carmelina Ave., Los Angeles, CA 90064, USA; britneys@ucla.edu Received 2010 July 26; accepted 2010 August 28; published 2010 October 11

ABSTRACT

Triton is one of the few bodies in the solar system with observed cryo-volcanic activity, in the form of plumes at its south pole, which suggests large-scale surface volatile transport over time. Triton's large variations in obliquity have motivated prior predictions of changing atmospheric column densities of several orders of magnitude, driven by seasonal evaporation of surface volatiles. Using the $Hubble\ Space\ Telescope$, we directly imaged Triton's surface and have detected large-scale differences in increased and decreased reflectance when compared with $Voyager\$ data at UV, visual, and methane-band wavelengths. Our surface map shows regions of increased brightness at near-equatorial latitudes and near the Neptune-facing side, and darkened regions near longitudes of $\pm 180^\circ$, indicating the presence of ongoing seasonal volatile transport.

Key words: planets and satellites: individual (Triton) - planets and satellites: surfaces

1. INTRODUCTION

As on the Earth, Triton's obliquity (Harris 1984) drives seasonal temperature changes over its surface. The south-pole region undergoes a cycle of seasonal excursions over the course of each of Neptune's orbits, i.e., an over period of 164.8 years. The extremes in the sub-solar latitude vary between successive summer solstices, due to the combination of the satellite's own orbital inclination with respect to Neptune, and Neptune's own orbital inclination (Harris 1984). Our current epoch (2000–2020) represents a period of extreme seasonal change on Triton.

Seasonal extremes initiate the transport of volatiles over Triton's surface by sublimation over more illuminated regions and re-deposition over less illuminated regions that act as cold traps (Trafton 1984). Since 1990, spectroscopic observations from 0.8 to 2.5 μ m have shown the surface composition to be dominated by solid nitrogen, along with methane and water, and containing trace constituents of CO and CO₂ that vary in abundance over leading and trailing longitudes (Quirico et al. 1999; Grundy & Young 2004). The average sub-solar ice temperature over Triton's disk is near 36.5 ± 1.5 K (Grundy & Young 2004), but with reflectance variations between 0.9 and 0.7 (Hillier et al. 1994), localized dark areas receive a threefold increase in energy from the average surface that can increase the temperature to 42 K and initiate a rapid increase in the sublimation of solid nitrogen off the surface.

In 1989, the brief Voyager 2 encounter with Triton revealed a dynamic surface, with varied regional terrains. The dramatic observation of active plumes emanating from the southern-most terrain was accompanied by imaging of a bright collar at mid-latitudes that transitioned to a darker cantaloupe terrain further northward. These features have been interpreted as seasonally variable (Kirk et al. 1995), owing to the near-solstice time of the spacecraft encounter. The solar illumination of the south pole reaches its highest intensity only once in a millennium, most recently in June of 2000. Our own observations obtained in June of 2005 are the most recent imaging observations of Triton and are the closest to follow this rare summer solstice event. Our

derived surface maps and photometry provide evidence that the surface of this satellite has undergone significant change since the *Voyager 2* encounter that is attributable to seasonally induced volatile transport.

2. OBSERVATIONS

The results from long-term monitoring of Triton from the ground (Buratti et al. 2006) motivated us to observe Triton using the Hubble Space Telescope's (HST's) Advance Camera for Surveys (ACS). HST had the best optical resolution available for imaging and the best response for UV photometry. The ACS High Resolution Camera (HRC) mode afforded the smallest pixel size (0'.028-0'.025), and with Triton's angular diameter of nearly 0.13 arcsec in size, resulted in an approximately 5 x 5 pixel image of Triton's surface. We observed a complete sampling of Triton's rotation period of 5.9 days to produce a photometric light curve. The observations took place over the time period from 2005 June 15-20 at approximately 23 hr intervals, yielding six samplings of sub-observer longitudes. The phase angle interval we observed over, from 1°55 to 1°45, was a well-behaved and well-sampled region of Triton's phase response, external to the narrow opposition surge (Buratti et al. 2006) and with a less than 0.005 mag variation over the entire span (Goguen et al. 1989).

Observations were made through available filter bandpasses similar to those of previous observations, in the ultraviolet (HST-ACS filter F220W), at approximate Johnson B (F435W), V (F555W), and R (F775W) bandpasses, and near the 890 nm methane-band (F892N). At each visit, two 75 s exposures were made through the F555W filter, two 60 s exposures through F775W, two 140 s exposures through F435 W, a 500 sexposure in F892N, and a 600 s exposure through the F220W filter. Table 1 summarizes the viewing geometries and V-band magnitudes for each visit.

3. RESULTS AND ANALYSIS

We used the HST standard pipeline product images for our analysis, processed up through cosmic-ray spike filtering

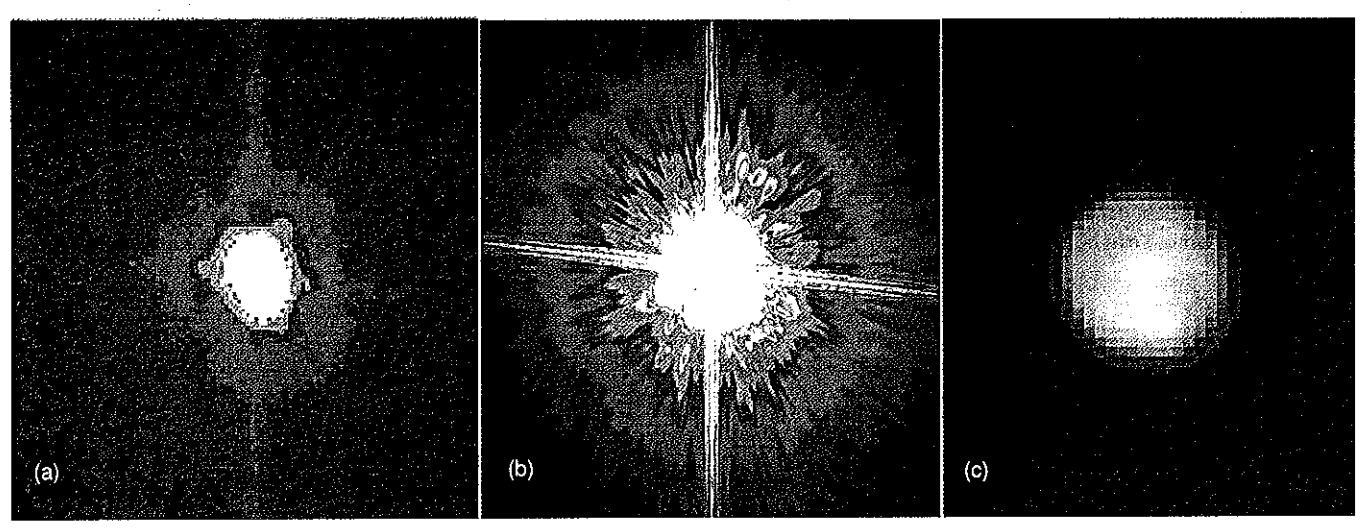


Figure 1. HST ACS—HRC image deconvolution process. Panel (a) shows a pipeline-processed image of Triton, cleaned of pixel defected and cosmic rays. Panel (b) shows the input PSF model for the same Triton image data, oversampled by four times the pixel scale of the original HST image data. Panel (c) is the resultant oversampled image of Triton's surface.

Table 1
Triton HST Observing Summary

Visit Start Date and Time (UT)	Observer IAU Triton East-longitude and Latitude at Visit (°)	Phase Angle (°)	V-band Magnitudes $(R = 30.06 \text{ AU}, \Delta = 29.4 \text{ AU})$
2005-06-15, 15:38	167.3, -48.9	1.55	13.625 ± 0.001
2005-06-16, 15:37	228.5, -48.9	1.53	13.639 ± 0.001
2005-06-17, 15:36	289.7, -48.9	1.51	13.629 ± 0.001
2005-06-18, 13:59	346.8, -48.9	1.49	13.597 ± 0.001
2005-06-19, 13:59	48.0, -48.9	1.47	13.594 ± 0.001
2005-06-20, 12:22	105.1, -48.9	1.45	13.609 ± 0.001

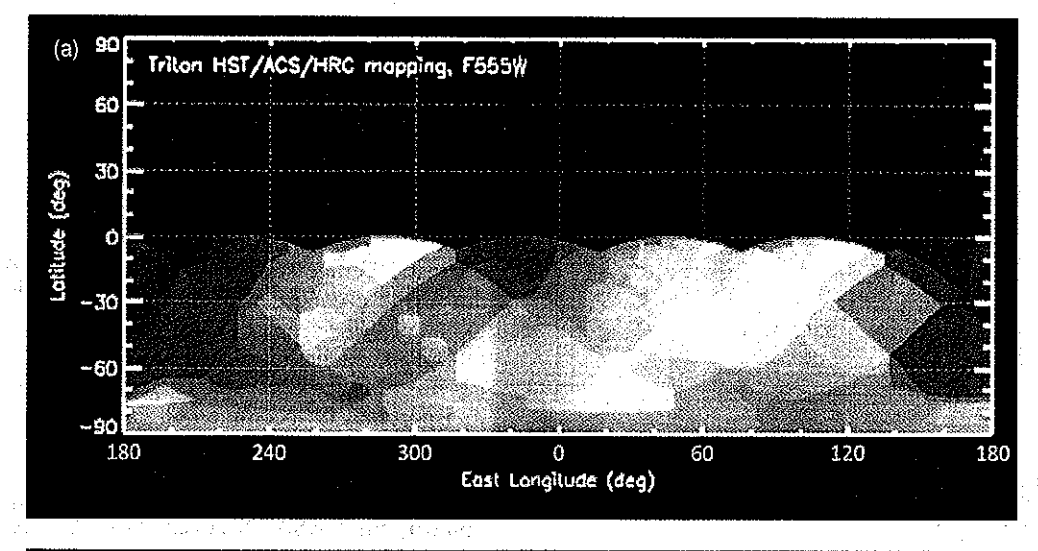
on each of the images. This standard pipeline calibration accounts for biasing and dark levels, the gain of the CCD on pixel scales, and aberrations of the optical system, thereby greatly simplifying the image reduction process and improving photometric accuracy. An example of a final image is shown in Figure 1(a). Instrument calibration data are updated routinely to account for changes to the telescope and detectors over time. We checked our pipeline-reduced images for saturation, but our exposure times were sufficiently short that the peak values on Triton's center were under half the saturation limit of the ACS-HRC for every frame.

An aperture photometry technique was used to extract signal counts from the frames. To derive each magnitude point, we measured the signal out to 2 arcsec from Triton's center and selected several background regions greater than 3 arcsec away from Triton, but at similar distances from Neptune as Triton. Any residual cosmic rays that remained in the regions of interest after pipeline processing were removed individually prior to the aperture photometry using IRAF package subroutines (Tody & Fitzpatrick 1996) that interpolate between unaffected pixels. We derived Triton's surface-reflectance values from the images using the size of the satellite reported from the Voyager 2 encounter (radius 676.3 km; Thomas 2000). We then corrected to mean Neptune distances (a heliocentric distance of 30.06 AU and an observer distance of 29.4 AU).

After the F555W images were reduced, we applied the Maximum Entropy Minimization (MEM) deconvolution method (Wu 1995) to the image set. We selected this band because of its high signal-to-noise, and because surface contrast between volatile-rich and volatile-poor regions is high in this spectral region. The MEM technique uses a model point-spread function (PSF) as

input to redistribute the detected photons according to the way the *HST* and ACS-HRC distributes the light. Because the *HST* and its instruments are well characterized and stable observing systems, unaffected by atmospheric variations, the PSF is very stable over long timescales. However, the PSF varies slightly depending on where the object of interest is imaged by the optics and its location on the detector, so that the model PSF must be generated for each image. We used the Tiny Tim package (Krist 1993) developed for *HST* observing and maintained by the Space Telescope Science Institute to generate PSFs for the individual images (Figure 1(b)). The Triton images were oversampled by a factor of four, matching the PSF model sampling, in preparation for deconvolution. The PSF model and image were then input to the MEM routine to generate a deconvolved image of Triton (Figure 1(c)).

A map of Triton's surface was generated from the resultant images using similar methods employed by the co-authors on observations of other small bodies by HST (Li et al. 2006; Schmidt et al. 2009). Pixels containing Triton's limb were discarded while the remaining pixels were mapped to an east-longitude/latitude grid. Overlapping pixels were median filtered, and the resultant image was smoothed over a moving 7.5×7.5 square area of the map (Figure 2(a)) to minimize any pixel-to-pixel noise effects introduced by the overlap averaging. For comparison, a map of the Voyager 2 Green-filter images was created over an identical grid and is shown at similar contrast (Figure 2(b)). The Voyager 2 Green filter bandpass is comparable to that of the HST F555W filter. The regions of Triton's surface that were observed by HST in 2005 and by Voyager 2 were very similar. The Voyager 2 fly-by afforded views of the full range of longitudes at a sub-solar latitude of -45° .4 during the



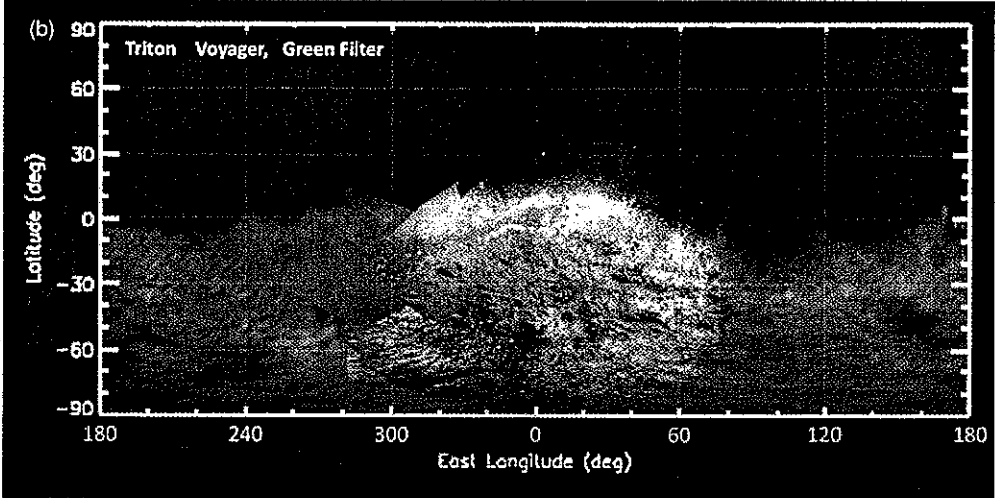


Figure 2. Comparison of Triton's surface as observed by HST in 2005 (Panel (a)) and during the Voyager 2 encounter (Panel (b)) at similar wavelengths. Panel (a)'s image has been smoothed to match HST's non-deconvolved imaging resolution (~0.05 arcsec) at the central wavelengths of 540 nm.

encounter. The *HST* images also sampled the entire range of longitudes when the sub-solar latitude was a similar -49°2.

The reflectance values derived from the magnitude values of Triton in the photometry reduction are shown in Figure 3(a), along with the *Voyager* 2 encounter light curves (Hillier et al. 1991). The *HST* light curve features correspond well with the image maps of the same observations. Figure 3(b) shows the light curve amplitudes in the F555W and F892N (methane) bands relative to the predicted amplitudes at the same epoch of the *HST* observations as projected from the *Voyager* 2 encounter imaging data (Hillier et al. 1991). The figure also includes observations in these two bands at other epochs for comparison. The mean reflectance values through each of the *HST* filters were 0.51 ± 0.02 (F220W), 0.67 ± 0.01 (F435W), 0.74 ± 0.01 (F555W), 0.88 ± 0.01 (F735W), and 0.73 ± 0.02 (F892N), and are similar values to those found in the literature at analogous filter wavelengths (Hicks & Buratti 2004; Young & Stern 2001).

4. DISCUSSION

The HST map shows a marked change in albedo patterns when compared to the Voyager imaging observations obtained 16 years earlier. This finding suggests the substantial transport

of surface frost during Triton's recent southern summer solstice. A large high albedo region near 180° longitude darkened significantly, while a region near the equator at 60° and possibly at 280° brightened (see Figure 2). These patterns imply transport of volatiles from the caps toward the equator, while the sub-solar latitude changed from -45° during the *Voyager* 2 encounter to -49° at the time of our *HST* observations after reaching a solstice minimum latitude of -50° in late 2000. One deficiency in both the *Voyager* and *HST* data is the lack of data north of the equator: it is unknown whether there is a northern polar cap that acts as a cold trap and is growing during this period of frost migration.

The rotational light curves provide clues to the identity of the transported frost. The brightest visible regions are also the darkest in the UV $(0.22 \,\mu\text{m})$; the frost must have an absorption band between 0.44 and 0.22 μ m, as well as have high vapor pressures at the surface temperature of Triton. H₂O and CO₂ remain solid at Triton's surface throughout its full seasonal cycle. The spectrum of N₂ ice is relatively featureless at visual-band wavelengths (Yelle et al. 1995). Considering its relatively high vapor pressure at Triton's distance (Brown 2000), N₂ remains the most likely candidate species for driving seasonal volatile transport (Elliot et al. 1998). The light curve in the methane absorption band at 0.89 μ m (filter F892N)

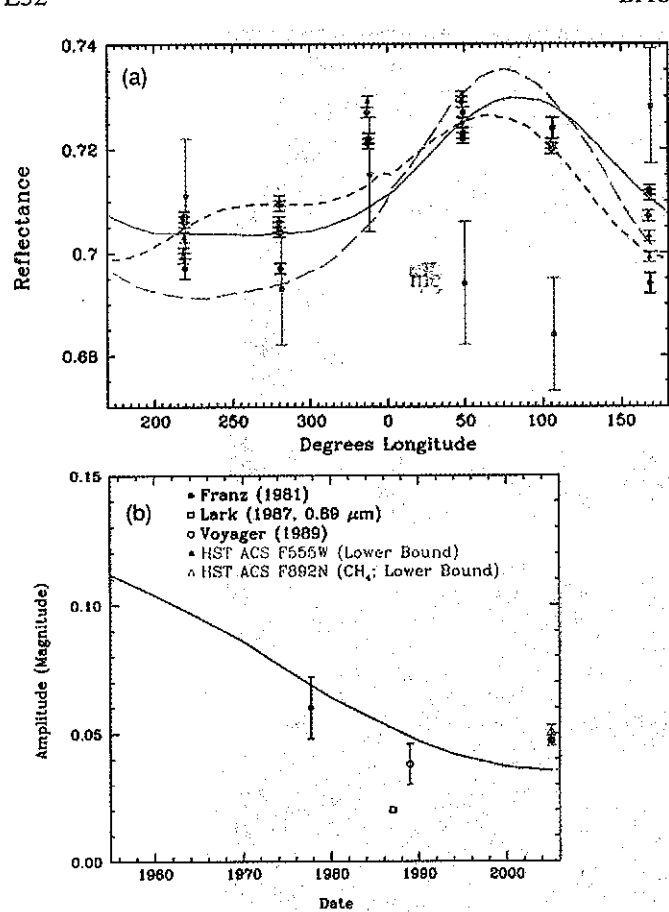


Figure 3. Comparative light curve amplitudes of the HST and Voyager 2 encounter data. (a) The reflectance light curves of the HST data in the F220W (magenta circles), F435W (blue squares), F555W (green diamonds), F775W (red triangles), and F892N (black circles) filter bands. The light curves derived from the Voyager 2 encounter data in three bands are shown as well; the UV (long-dashed magenta line), blue (short-dashed blue line), and the green (solid green line). All the data have been shifted to the F555W band's mean reflectance for comparison. (b) The amplitude of the light curves derived from the 2005HST observations (red) and the values in the literature. Except for the Lark et al. (1989) data (open square), the other points from the literature (Hillier et al. 1991; Franz 1981) are for V-band observations, similar to the HST F555W band. The Lark data were taken through a methane band similar to the HST F892N filter. The solid line is the predicted magnitude of Triton's light curve (Hillier et al. 1991) based on the surface map from the Voyager 2 encounter. The amplitude changes with time due to the change in time of the sub-solar latitude on Triton.

shows a pronounced minima coincident with the darker regions at 0.55 μ m (filter F555W). As lower brightness at 0.89 μ m corresponds to the presence of more exposed CH₄, this is consistent with possible denuding of methane ice in the darker regions of the surface seen at 0.55 μ m.

Evidence for seasonal volatile transport is also provided by stellar occultation measurements of Triton's atmosphere that show an increase in temperature during the 10 years after the *Voyager 2* encounter that implies a doubling of its atmospheric bulk (Elliot et al. 1998). Sublimation of solid nitrogen down to depths of millimeters over a few percent of the surface would increase atmospheric pressure significantly. An *HST* map obtained in 1995 shows an extensive region near longitude 340° that darkened and reddened in the visible (0.28–0.41 μm; Flynn et al. 2001), and earlier *HST* observations suggested volatile

transport on Triton (Young & Stern 2001). Triton also exhibits variations in the depth of its methane band at 0.89 μ m (Hicks & Buratti 2004), further evidence that the transport or exposure of methane is occurring. Finally, the strength of the 2.15 μ m nitrogen band is decreasing, particularly in the Neptune facing hemisphere (Grundy et al. 2010).

Volatile transport has recently been detected on Pluto (Buie et al. 2010), which is also expected to undergo seasonal changes in frost coverage similar to those on Triton but more extreme due to its eccentric orbit and obliquity. It is thus important to characterize seasonal volatile transport on these two bodies as typical of what may be happening on Kuiper Belt objects in general. Our work presented here suggests that seasonal volatile transport may be a common ongoing process on the larger solid bodies at these heliocentric distances.

Funding for the analysis of the *Voyager* images was provided in part by the NASA Discovery Data Analysis Program. The research presented was partially based on observations made with the NASA/ESA *Hubble Space Telescope*, the analysis of which was funded through a grant from the Space Telescope Science Institute. STScI is operated by the association of Universities for Research in Astronomy, Inc. under the NASA contract NAS 5-26555.

REFERENCES

Brown, M. E. 2000, AJ, 119, 977

Buie, M. W., Grundy, W. M., Young, E. F., Young, L. A., & Stern, S. A. 2010, A.,

Buratti, B. J., Bauer, J., Hicks, M., Herbert, B., Schmidt, B., Cobb, B., & Ward, J. 2006, American Geophysical Union Spring Meeting, P33A-02

Elliot, J. L., et al. 1998, Nature, 393, 765

Flynn, B., Stern, S. A., Trafton, L., & Stansberry, J. 2001, Icarus, 150, 297

Franz, O. G. 1981, Icarus, 45, 602

Goguen, J. D., Hammel, H. B., & Brown, R. H. 1989, Icarus, 77, 239

Grundy, W. M., & Young, L. A. 2004, icarus, 172, 455

Grundy, W. M., Young, L. A., Stansberry, J. A., Buie, M. W., Olkin, C. B., & Young, E. F. 2010, Icarus, 205, 594

Harris, A. W. 1984, NASA Conf. Publication, Uranus and Neptune (N85--11927 02--91) 357

Hicks, M. D., & Buratti, B. J. 2004, learns, 171, 210

Hillier, J., Veverka, J., Helfenstein, P., & Lee, P. 1994, Icarus, 109, 296

Hillier, J., Veverka, J., Helfenstein, P., & McEwen, A. 1991, J. Geophys. Res., 96, 19211

Kirk, R. L., Soderblom, L. A., Brown, R. H., Keiffer, S. W., & Kargel, J. S. 1995, in Neptune and Triton, ed. D. P. Cruikshank (Tucson, AZ: Arizona Press), 949

Krist, J. 1993, in ASP Conf. Ser. 52, ADASS II, ed. R. J. Hanisch, R. J. V. Brissenden, & J. Barnes (San Francisco, CA: ASP), 536

Lark, N., Hammel, H. B., Cruikshank, D. P., Tholen, D. J., & Rigler, M. A. 1989, Icarus, 79, 15

Li, J.-Y., McFadden, L. A., Parker, J. W., Young, E. F., Stern, S. A., Thomas, P. C., Russell, C. T., & Sykes, M. V. 2006, Icarus, 182, 143

Quirico, E., Doute, S., Schmitt, B., de Bergh, C., Cruikshank, D. P., Owen, T. C., Geballe, T. R., & Roush, T. L. 1999, Icarus, 139, 159

Schmidt, B. E., et al. 2009, Science, 326, 275

Thomas, P. C. 2000, learns, 148, 587

Tody, D., & Fitzpatrick, M. 1996, in ASP Conf. Ser. 101, ADASS V, ed. G. H. Jacoby & J. Barnes (San Francisco, CA: ASP), 322

Trafton, L. 1984, Icarus, 58, 312

Wu, N. 1995, in ASP Conf. Ser. 77, ADASS IV, ed. R. A. Shaw, H. E. Payne, & J. J. E. Hayes (San Francisco, CA: ASP), 305

Yelle, R. V., Lunine, J. I., Pollack, J. R., & Brown, R. H. 1995, in Neptune and Triton, ed. D. P. Cruikshank (Tucson, AZ: : Arizona Press), 1031

Young, L. A., & Stern, S. A. 2001, AJ, 122, 449